Journal of Engineering in Industrial Research

2024, Volume 5, Issue 2

Original Research Article

Microstructural and Mechanical Properties of Heat-Treated Low Carbon Steel Welded with Varied Joint Designs

Isiaka Oluwole Oladele[1], Samuel Olumide Falana[1,*], Collins Chidiebere Okoye[1], Peace Pamilerin Adara[1], Adesuyi Kole Aladenika[2, 3], Sunday Gbenga Borisade[4]

[1]*Department of Metallurgical and Materials Engineering, Federal University of Technology, PMB 704, Akure, Ondo State, Nigeria*
[2]*Department of Science Laboratory Technology, Rufus Giwa Polytechnic Owo, Ondo State, Nigeria*
[3]*Department of Physics, Federal University of Technology, PMB 704, Akure, Ondo State, Nigeria*
[4]*Department of Materials and Metallurgical Engineering, Federal University Oye, Ekiti State, Nigeria*

Citation I.O. Oladele, S.O. Falana, O.C. Chidiebere, P.P. Adara, A.K. Aladenika, S.G. Borisade. Microstructural and Mechanical Properties of Heat-Treated Low Carbon Steel Welded with Varied Joint Designs. *J. Eng. Ind. Res.* **2024**, 5 (2):116-135.

https://doi.org/10.48309/JEIRES.2024.2.5

Article info:
Submitted: 2024-09-07
Revised: 2024-11-12
Accepted: 2024-12-07
ID: JEIRES-2409-1128

Keywords:
Low carbon steel; Weld joints; Oil bath; Post weld treatment; Shielded metal arc welding

ABSTRACT

This study examined the effects of joint design and post-weld heat treatment (PWHT) on the microstructural features and mechanical properties of low-carbon steel welded using the shielded metal arc welding (SMAW) process. Three joint configurations—bevel, butt, and half-lap—were welded under consistent parameters, with a subset of samples subjected to PWHT involving quenching in either used or unused oil baths. Mechanical testing, including tensile, hardness, and impact toughness tests, was conducted on both as-welded (AW) and PWHT-treated samples. Results showed that bevel joints exhibited the highest tensile, yield, and impact strengths, while butt joints demonstrated superior hardness. PWHT, particularly quenching in unused oil, significantly enhanced tensile strength, yield strength, and hardness, whereas quenching in used oil achieved the highest impact strength. Microstructural analysis of the bevel joints after quenching in unused oil, along with mechanical testing for tensile strength, yield strength, hardness, and impact toughness, revealed that PWHT notably improved mechanical performance compared to AW conditions. The bevel joints exhibited significantly higher tensile and yield strengths, as well as enhanced hardness, indicating the formation of a refined martensitic structure due to the quenching process. The study concluded that the choice of joint design and quenching medium can optimize welded joint properties for specific industrial applications. Bevel joints were recommended for high tensile and yield strength, whereas butt joints were preferable when hardness and toughness were essential.

***Corresponding Author: Samuel Olumide Falana** (olumide706@gmail.com)*

Introduction

Joining of materials is a crucial process in manufacturing and industrial sectors, which allows for intricate designs, enhances material utilization, and improves product performance. Welding is a crucial process in modern manufacturing, particularly in large-scale production. It simplifies maintenance and repair tasks, enhancing product durability and cost efficiency. The methods of joining materials include riveting, brazing, soldering, fastening, and welding, which create elaborate designs and intricate structures with either temporary or permanent joints. Among these methods, welding stands out as the most commonly employed in diverse manufacturing industries such as construction, automotive, shipbuilding, and aerospace due to its superior joint efficiency, straightforward arrangement, versatility, and cost-effectiveness, as well as the structural integrity it provides [1-3]. Unlike other methods of joining that aim to create a single component, welding processes are specifically utilized to bring together various components in order to achieve a desired intricate configuration [4]. While there are many different welding techniques used for joining steels, the most widely used ones include electric arc welding (EAW), gas shielded arc welding (which includes metal inert gas and metal active gas welding MIG/MAG, sometimes referred to as gas metal arc welding (GMAW), tungsten inert gas welding (TIG), also known as gas tungsten arc welding (GTAW), and submerged arc welding (SAW).

The EAW, also known as SMAW is known for its simplicity and portability, making it ideal for field applications and repairs where equipment mobility is crucial [5]. SMAW does not require external shielding gas, which can be a logistical advantage in outdoor or windy conditions. However, it generally exhibits lower deposition rates compared to GMAW and TIG welding. GMAW can achieve higher productivity due to its continuous wire feed mechanism, allowing for faster welding speeds and higher deposition rates [6]. In contrast, TIG welding offers superior control over the weld pool, produces high-quality welds, is slower, and requires more skill, leading to lower deposition rates than both SMAW and GMAW [7]. SMAW has several advantages, including its low cost, ease of use, and versatility in various positions and environments. However, its disadvantages include a higher likelihood of defects due to the need for slag removal and the potential for increased porosity in the welds compared to GMAW and TIG [6]. GMAW provides a cleaner weld with less post-weld cleaning required, as it uses a shielding gas to protect the weld pool from atmospheric contamination [7]. This process is also more efficient in terms of heat input, leading to finer grain structures in the weld metal (WM), which can enhance mechanical properties [8]. However, GMAW requires a more complex setup and is less effective in outdoor conditions unless specific precautions are taken [5]. TIG welding is renowned for producing high-quality welds with excellent aesthetic finishes and minimal distortion. It allows for precise control over the heat input and filler material, making it suitable for thin materials and critical applications [7]. However, this process is slower and more labor-intensive, requiring skilled operators, which can increase production costs [9]. SAW is characterized by its high deposition rates and deep penetration, making it ideal for thick materials and large-scale industrial applications. It is often used in shipbuilding and heavy fabrication due to its efficiency and ability to produce high-quality welds with minimal fume generation [10]. However, SAW is limited to flat or horizontal positions and requires a more complex setup, which can be a disadvantage in certain applications [5].

Given these considerations, this investigation is centered on EAW as the predominant welding method, also sometimes known as SMAW due to its advantages in terms of cost-effectiveness, ease of use, and suitability for the specific applications involving low-carbon steel, particularly in environments where mobility and simplicity are essential. It has found application in not only in aerospace, but also in automobile and home appliances [11-13]. To achieve high quality weld, many parameters must be taken into account. Factors such as time,

temperature, electrode characteristics, pulse frequency, power input, welding speed, current magnitude, voltage utilization, the type of welding filler, and the length of the arc are all crucial considerations [1,14]. Another crucial factor that must also be taken into consideration is the type of weld joint that will be used, based on the specific application requirements. According to Oladele *et al.* [3], inadequate joint design can undermine even the most optimal welding conditions. Therefore, a key aspect of weld joint design, particularly in arc welding, is ensuring sufficient accessibility and maneuvering space for the welding electrode or filler metal to facilitate the proper formation of weld beads. This study encompassed different types of weld joints, including butt joints, half-lap joints, and bevel joints. However, joint is employed for the purpose of connecting two components that are in alignment within the same plane. This particular type of joint finds frequent application in the realm of plates, sheet metal, as well as pipe work, more importantly, in situations where a considerable degree of strength is deemed necessary [4]. On the other hand, the bevel joint necessitates the prior shaping of metal edges prior to welding, a process that serves to establish a robust and uniform joint. The configurations of these grooves or shapes may assume different forms, such as straight, slanted, or V-shaped, featuring various angles that fall within the range of 8 to 50 degrees. The selection of the specific angle depends on the precise requirements of the given task. Furthermore, in the context of a half-lap joint, a certain amount of material is extracted from each of the components involved, resulting in a joint that matches the thickness of the thickest part. This particular characteristic enables welding to be conducted with a reduced level of constraints in terms of joint fit-up tolerances [3].

SMAW can be used to weld various types of steel as reported by previous researchers [13]. However, aluminum, nickel, and copper alloys can also be welded with this method. Steel, as the primary material examined in this research, was chosen due to its versatility and excellent weldability, thereby, minimizing the risk of brittle phase-induced cracking [15]. Its diverse applications span across construction, shipping, automobile, and aerospace industries. Classification based on carbon content categorizes steels into low (up to 0.3% carbon), medium (0.3-0.6% carbon), and high (above 0.6% carbon) carbon steels. Low carbon steel or mild steel, is renowned for its weldability at ambient temperature and this is because according to Ismael [16], the higher the carbon content, the lower the weldability. Low carbon content renders the possibility of the martensite phase formation in the HAZ extremely low. Therefore, many of the low carbon steels are easy to weld, making it a popular choice in structural steel fabrication and assembly. Examples of weldable low carbon steels as graded by the american iron and steel institute (AISI) are AISI1010, AISI1018, AISI1020, and A36 [13,17] with AISI1020 being the steel of focus in this study. In service, it has been found that welded joints typically demonstrate weaker mechanical properties. This is due to the rapid heating and cooling process during welding, which results in the generation of residual stresses in the metal. In addition, there are changes in the microstructure, chemical composition, and surface composition of the welds and adjacent base metal. Work hardening occurs in the fusion zone because of solute segregation or grain coarsening, further affecting the mechanical properties of low carbon steel [18-21]. Samir suggested that controlling the heating and cooling rate during welding is challenging, leading to a lack of complete control over the adverse effects on mechanical properties that ultimately results in weldment failure in service [21]. Hence, it is expected that any weld design should prioritize the preservation of the weld's integrity and the efficient reduction of weld defects. Metallurgists and Engineers have taken the lead in exploring methods to create optimal weld joints tailored to specific engineering applications, with the goal of preventing abrupt failures [18,22].

Heat treatment which is the process used to modify or enhance certain material properties by heating to a specific temperature, holding at that temperature, and then appropriately cooling to ambient temperature has been used extensively in this regard. This treatment is commonly utilized on weld joints, where it is referred to as PWHT. PWHT helps to decrease

segregation and change the microstructure of the weldment. In line with Oladele *et al.* [18], PWHT stands out as a valuable technique for strengthening joints by making adjustments to the size, shape, and distribution of secondary strengthening particles. Furthermore, according to Adebare and Edward [22] PWHT is defined as any heat treatment given after welding that is typically used to improve the properties of a weldment, with the primary purpose of providing stress relief, as stated in Harati *et al.* [23]. The primary benefits of PWHT are twofold: a large reduction in tensile residual stresses and, to a lesser extent, tempering of the heat affected zone and WM microstructures. This reduction in residual stresses and tempering enhances weld integrity by reducing the chance of fracture due to cold cracking. There are numerous heat treatment procedures, but weld joint annealing, normalizing, quenching, and stress relieving are the most commonly employed. The usage of annealing is limited due to grain growth which tends to reduce the mechanical strength of the weld junction. Normalizing and stress relief are common techniques in the process equipment fabrication sector. However, local stress relief is done with caution to avoid uneven heating and overheating. Normalizing produces a stress-free weld connection with a rather stable structure [21,24]. PWHT has been noted to cause different impacts on the characteristics of the welded joint due to influences by variables like the steel's chemical composition, the welding technique applied, and the specific type, duration, and temperature of PWHT utilized. Aninda *et al.* [25] consider the mechanical and microstructural properties of weld joint between mild steel plates before and after undergoing heat treatment process. The findings revealed that PWHT led to a 4.1% enhancement in tensile strength, a 13.84% increase in yield strength, and a 4.96% rise in percentage elongation. However, the hardness value decreased by 19.19% after heat treatment, indicating improved ductility of the specimen. Furthermore, a finer grain size, reduced grain gaps, and fewer voids were observed in the region of the EAW joint. In another research conducted by Osunbunmi *et al.* [26] where the impact of heat treatment on the mechanical and microstructural characteristics of low carbon steel is investigated. Analysis through optical microscopy indicated that heat-treated samples exhibited varying proportions of ferrite and pearlite. Among the samples, the annealed one displayed the most refined microstructure. The sample treated with hardening demonstrated the highest Brinell's Hardness number (BHN) of 434 BHN, while the annealed sample showed the highest toughness and ductility with an impact energy of 65.43 J. Comparatively, the microstructure of the heat-treated samples exhibited finer grain structures than that of the untreated control sample. Hence, judicious selection of heat treatment methods offers a valuable strategy for enhancing the microstructure of low carbon steels to achieve superior mechanical properties. Impact of PWHT on the hardness and microstructure of low carbon steel was also investigated by Adebare & Edward [22]. The samples that were welded underwent normalizing, annealing, and quench hardening in various substances such as water, palm oil, Quartz 5000 Total Engine oil, and Groundnut oil. After preparation, the samples (both PWHTs and as-welds) were tested for hardness and microstructure. A comparison was made with non-heat treated as-weld to analyze their hardness and observed microstructure. The results displayed significant variations in the microstructure and mechanical properties among the different PWHT samples.

Furthermore, the performance and application of the joint designs considered in this research—bevel, butt, and half-lap—differ significantly after undergoing PWHT. Each joint type exhibits unique mechanical properties and failure modes, influenced by their geometrical configurations and the nature of the welding process. Butt Joints characterized by their simple design, where two pieces are joined end-to-end, butt joints typically exhibit lower strength compared to bevel and half-lap joints due to a smaller bonding surface area, which can lead to adhesive failure under stress [27,28]. However, PWHT can significantly enhance the tensile strength and fatigue resistance of butt joints, particularly in low-carbon steels and aluminum alloys [3,29]. It is important to note that the presence of weld defects, such as undercuts, can severely compromise the fatigue

life of butt joints, making them less reliable in high-stress applications [30,31].

Bevel joints design allows for better stress distribution, leading to improved mechanical performance compared to butt joints. Research indicates that bevel joints exhibit higher transverse strength and reduced microleakage, attributed to the increased bonding area and the ability to better manage tensile and shear stresses during loading [32,33]. PWHT can further refine the microstructure and enhance the overall strength of bevel joints [3,29]. However, the effectiveness of PWHT varies depending on the specific material and joint configuration. While for half-lap joints which, provide a larger bonding area than butt joints, making them particularly advantageous in applications where shear strength is critical. They effectively distribute loads across a wider area [34]. The performance of half-lap joints can also improve through PWHT, enhancing fatigue resistance and overall durability [29]. Similar to bevel joints, the effectiveness of half-lap joints can be compromised by weld quality and the presence of defects, leading to premature failure under cyclic loading conditions [31,35].

In summary, while butt joints are simpler and easier to manufacture, they generally offer lower performance compared to bevel and half-lap joints, particularly after PWHT. Bevel joints provide better mechanical properties due to their increased bonding area and stress distribution capabilities, while half-lap joints excel in applications requiring high shear strength. Therefore, the choice of joint design should consider specific application requirements, including load conditions, environmental factors, and the potential for post-weld treatments.

While extensive research has been conducted on PWHT of low carbon steel, particularly focusing on annealing and normalizing, there remains a significant gap in understanding the quenching effects in oil media, especially when considering different welding joints. This research aims to fill this knowledge gap and enhance our understanding of oil quenching as a viable PWHT method. Specifically, this study investigates the mechanical properties (hardness, tensile and impact strengths) of three distinct weld joints—butt, half-lap, and bevel—before and after PWHT in both used and unused oil media. The objectives of this research are threefold which are; quantify the effects of oil quenching (in both used and unused oil) on the hardness, tensile and impact strengths of the different weld joints, compare the mechanical properties of the weld joints before and after PWHT to determine the optimal combination for specific applications and assess the feasibility and effectiveness of using used oil as a quenching medium, potentially offering a cost-effective and environmentally friendly alternative. The novelty of this research lies in its comprehensive examination of the impact of oil quenching on various weld joint configurations, utilizing both fresh and used oil to simulate real-world scenarios. By analyzing the resulting mechanical properties, the study provide valuable insights into the efficacy of oil quenching as a PWHT technique, potentially leading to improved welding practices and enhanced material performance in industrial applications.

Materials and Methods

For this study, hot-rolled low-carbon steel (8 mm thick) sourced from a steel industry in Sango-Ota, Ogun State, Nigeria was used. The base metal, an AISI 1020 type, is renowned for its high ductility, good machinability, moderate strength, toughness, and excellent weldability. An E6013 mild steel welding electrode with a nickel-potassium coating, suitable for both AC and DC welding, was sourced from a local vendor in Akure, Nigeria, and used in the welding process. Detailed chemical compositions are provided in Tables 1 and 2.

Table 1: Chemical composition of steel (AISI 1020 type)

Elements	C	Si	Mn	P	S	Cr	Mo	Ni	Al	Fe
Composition	0.199	0.212	0.522	0.0179	0.0096	0.0439	0.0029	0.0155	0.0407	98.98

Table 2: Chemical composition of electrode (E6013)

Elements	Fe	C	Mn	Si	P	Ni
Composition	Bal	0.12	0.3	0.35	0.04	0.035

Where, C=carbon; Si= Silicon; Mn=Manganese; P= Phosphorus; S= Sulphur; Cr= Chromium; Mo= Molybdenum; Ni-Nickle; Al; Aluminum; and Fe= Iron.

Experimental procedure

Low-carbon steel sheets with an 8 mm thickness were cut into sizes according to the joint design specifications, with a vice securely holding each piece to ensure precise and accurate cutting. The joint designs used were the butt joint, half-lap joint, and bevel joint. The butt joint was created by cutting the material vertically to dimensions of 50 × 50 × 8 mm, the half-lap joint was formed by machining a section of the material to 50 × 10 × 4 mm, and the bevel joint was produced by cutting the material at a 30° angle from the edge to the horizontal. Each cut sample was smoothed and thoroughly cleaned to remove impurities that could cause inclusions and affect the weld quality, thereby ensuring easier coupling during welding. The samples were then paired and aligned on a table using an angular iron, and the welding circuit was prepared before welding.

The welding process was conducted in a horizontal position using the SMAW method. A welding current of 110 A, a welding voltage of 23 V, and a welding speed of 3.57 mm/s were consistently maintained throughout. After welding, the welded joints were brushed to ensure complete penetration, and a wire brush was used to remove spatter and achieve a good surface finish. PWHT was conducted in two stages: quenching and tempering. The welded samples were divided into two groups and placed in a furnace pre-heated to 850°C. This temperature was chosen to facilitate the optimal austenitization of low-carbon steel (AISI 1020), which typically requires a temperature range of 800 to 900 °C to improve mechanical properties through quenching and tempering. The samples were soaked at 850°C for one hour to ensure uniform temperature distribution throughout the material [18]. After the soaking period, the furnace was switched off and kept closed to retain the heat.

Immediately after removing from the furnace, the first group of samples was quenched in an unused oil bath at room temperature for exactly 5 minutes, while the second group was quenched in a used oil bath, also at room temperature, for 5 minutes. The cooling rates in both media were measured to be approximately 30 °C/s. The unused oil, characterized by its lower viscosity and higher thermal conductivity, allowed for a more rapid cooling rate, which promoted the formation of finer martensitic structures. In contrast, the used oil, which contained contaminants from prior automotive use, had a higher viscosity and thermal degradation, likely affecting the cooling rates and, subsequently, the mechanical properties of the welded joints. Following quenching, both groups of samples were immediately returned to the closed furnace, which remained at 280 °C without reheating, to undergo tempering. The samples were left in the furnace to cool gradually to room temperature, thereby reducing residual stress and minimizing the risk of cracking.

Mechanical evaluation and microstructural characterization

The mechanical tests that were carried include the tensile, impact and hardness test. A Universal Testing Machine was used to perform the tensile tests on the samples. The ends of the test samples were secured in grips connected to a straining device and a load measuring device. Upon fracturing of the test sample, the results were generated by computer software.

The Izod impact test was conducted on the samples using a Honfield Balance Impact Testing Machine in accordance with american society

for testing and materials (ASTM) E23. Prior to mounting on the machine, the test samples were notched to a depth of 2 mm with a V-shaped hand file. The notched test samples were then mounted on the impact testing machine, which applied a constant impact force. The amount of impact energy absorbed by the specimens before yielding was read from the calibrated scale on the impact testing machine.

The hardness of the base metal, heat-affected zone (HAZ), and WM across the welded joint of the samples was measured using a digital Vickers micro-hardness tester, specifically an Indentec-Hardness Testing Machine, according to ASTM E92-17 at 5 mm intervals from the WM. Hardness testing was conducted across regions of the welded joint that are typically impacted by welding and PWHT, specifically near the weld centerline and within the HAZ. Although specific test lines were not precisely marked, these areas were chosen to provide insights into variations in hardness as influenced by different joint designs and cooling rates. Future work could improve upon this by marking exact test locations for more accurate and replicable measurements across samples. The specimens were ground using various grades of emery paper (220, 320, 500, 600, 800, and 1000), followed by polishing and etching procedures. In accordance with ASTM E407-3, the polished surfaces were etched with Keller's reagent (2 mL HNO_3 + 3 mL HCl + 5 mL HF + 150 mL H_2O) for approximately 18 seconds. Micrographs of the samples were obtained using a Nikon Optiphot metallurgical microscope and a Nikon D70 digital camera at magnifications of 100x. The examination of the microstructures in the weld zone (WZ), HAZ, and parent metal (PM) was conducted using optical microscopy, as demonstrated in Figures 1-3.

Results and Discussion

Microstructure analysis

The microstructural analysis, as illustrated in Figures 1-3 at 100x magnification, reveals a typical ferrite and pearlite microstructure. In Figure 1a, the micrograph displays lighter regions representing ferrite, while the darker, more etched areas correspond to pearlite. Ferrite, characterized by a body-centered cubic (BCC) structure, contributes to the ductility of the steel, whereas pearlite, a lamellar mixture of ferrite and cementite (Fe_3C), enhances its strength. The grains are relatively uniform and elongated, indicative of rolled low-carbon steel, with visible grain boundaries suggesting etching. This microstructure indicates that the steel exhibits both ductility and toughness, balanced by the strength provided by pearlite. The presence of pearlite colonies and uniform ferrite grains suggests that the material cooled from the austenite phase. The 20-micrometer scale bar aids in assessing grain size, confirming that the sample preparation, including etching and polishing, was properly executed. Overall, the microstructure indicates that the steel possesses desirable mechanical properties suitable for various applications.

Likewise, Figure 1b shows the micrograph of the HAZ in low-carbon steel (AISI 1020) after welding. It provides crucial insights into the structural changes induced by the welding process. The image shows a more pronounced and coarser microstructure compared to the base metal, indicative of the transformations due to thermal cycles experienced during welding. The darker regions represent cementite formation, resulting from the rapid cooling rates in the HAZ. Cementite is a hard and brittle phase, which significantly increases the hardness of the HAZ. The lighter regions observed represent the ferrite phases and are less prominent due to grain refinement. The observed microstructure, with its mixed phases, highlights the increased brittleness and hardness in the HAZ compared to the unaffected base metal; this can be linked to the hardness, as seen in Figure 1. This change can adversely affect the toughness of the material, making it more susceptible to fracture under stress. This detailed microstructural view underscores the importance of controlled welding parameters to manage HAZ properties and ensure the integrity of the welded joint.

Figure 1c illustrates the WM microstructure, which reveals a heterogeneous matrix composed primarily of ferrite, interspersed with Widmanstätten ferrite and acicular ferrite with

dark spots of cementite. The presence of these distinct ferrite morphologies indicates a complex thermal history during the welding process, characterized by varying cooling rates.

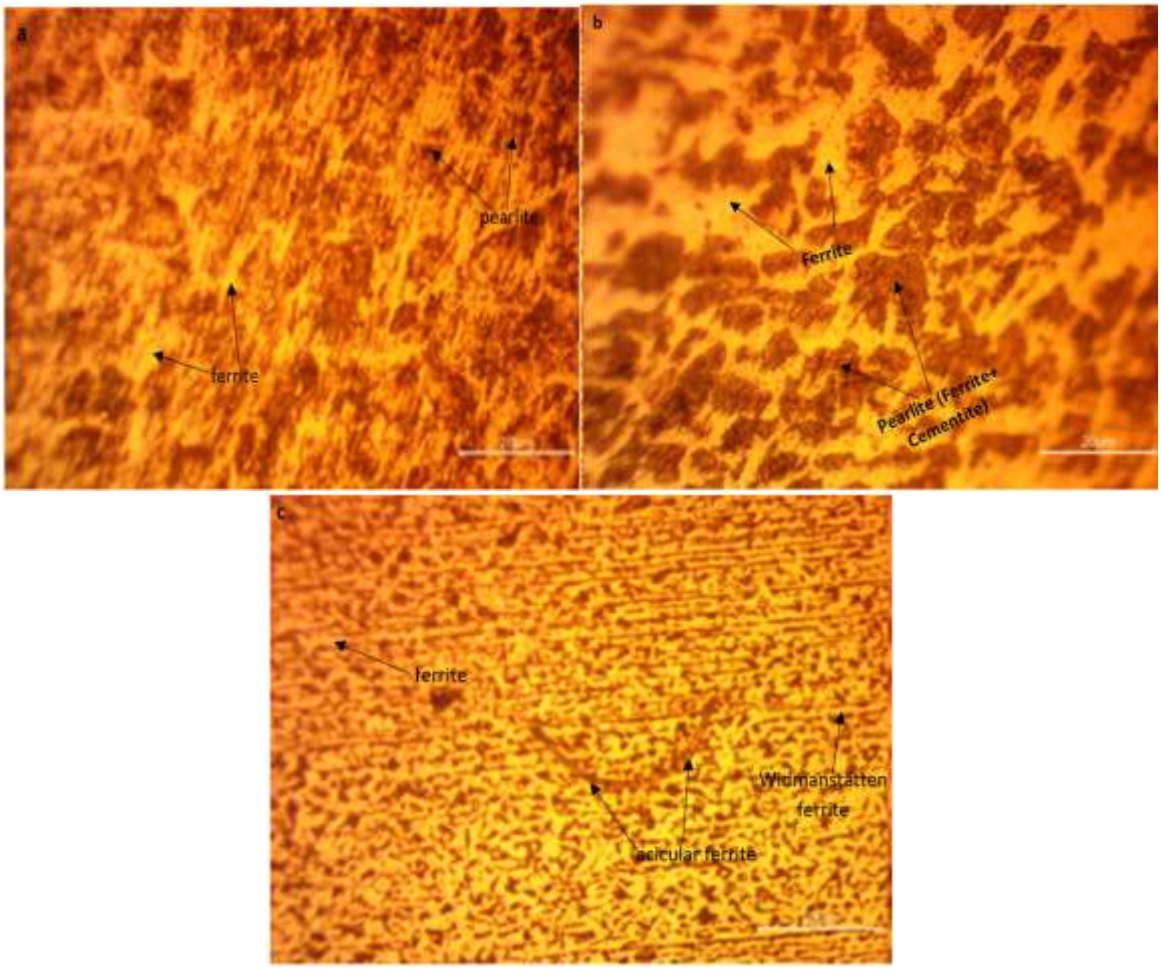

Figure 1: Optical micrograph (a) Base metal of welded low carbon steel. (b) HAZ of welded low carbon steel. (c) WM of welded low carbon steel

The predominant ferrite phase, with its relatively coarse grains, suggests moderate cooling rates, while the finer Widmanstätten and acicular ferrite structures are indicative of localized rapid cooling.

This intricate microstructure significantly influences the weld's mechanical properties, contributing to a balance of strength, toughness, and ductility. The ferrite matrix provides the foundation for ductility, while the Widmanstätten and acicular ferrite enhance strength and hardness. However, the presence of Widmanstätten ferrite can also introduce some susceptibility to brittle fracture under certain loading conditions, likewise that of the cementite.

Figure 2 illustrates the microstructure of the base metal, HAZ, and WM following quenching in a previously un-used oil bath. The microstructural examination of the base metal after PWHT (Figure 2a) provides valuable insights into the effects of quenching and subsequent slow cooling in the furnace on low-carbon steel.

The micrographs reveal distinct lighter and darker regions, illustrating the phase distribution and highlighting the effects of the heat treatment process. A predominantly fine-grained structure is observed, indicating a refined microstructure achieved by rapid quenching in unused oil for 5 minutes, followed by controlled furnace cooling at 280 °C to room

temperature. This gradual cooling process in the furnace provided a uniform rate of temperature reduction across the structure, unlike air cooling, which can induce high residual stresses due to differential cooling rates. When outer layers cool and contract more rapidly than inner layers, they create tensile stresses that pull on the warmer inner material, a common cause of cracking, especially in weld regions, which are structurally more vulnerable. By employing a controlled furnace cooling process, these internal stresses were minimized, helping to preserve the structural integrity of the welded joints. The predominant lighter regions as observed in the micrograph are ferrite, which is the primary phase in low-carbon steels due to their limited carbon content. The ferrite phase remains largely unaffected by quenching since the carbon content is insufficient to fully transform it into harder phases. As a result, these ferritic regions retain their characteristic light appearance in optical micrographs, indicating areas of lower hardness and high ductility. The darker regions observed are likely composed of fine pearlite or possibly bainite. The quenching process initiated a rapid transformation of austenite into these phases, as martensite formation is minimal in low-carbon steel due to the low carbon content. This darker region, which signifies the pearlite phase, can be associated with cementite due to its higher carbon concentration, thereby providing enhanced strength of the base metal after heat treatment. Following quenching, the sample, which was tempered at 280 °C, promotes carbide precipitation, as seen in Figure 2a, which is represented by much darker spots, leading to a reduction in brittleness and an improvement in ductility. At this relatively low tempering temperature, the structure of pearlite would become more stable, allowing for finer carbide dispersion within the ferric matrix. This contributes to increased toughness without significantly compromising hardness, creating a balanced microstructure suitable for welded applications where both strength and impact resistance are desired.

The micrograph in Figure 2b illustrates the microstructure of the HAZ in a PWHT low-carbon steel sample quenched in an un-used oil bath. The analysis also reveals a predominantly fine-grained structure, indicative of refinement from the PWHT process. These fine grains contribute to improved mechanical properties, such as increased toughness and strength. The needle-like or lath-shaped dark regions observed in the micrograph are likely bainitic phases formed at intermediate cooling rates between pearlite and martensite. These bainitic phases significantly increase hardness and strength. In addition, the presence of light regions indicates the presence of pearlite, a mixture of ferrite and cementite, and potentially ferritic phases (very light regions). This suggests that the cooling rate in the un-used oil was not fast enough to transform all austenite into the bainitic phase, as well as the carbon content of low-carbon steel. Furthermore, the PWHT might have led to the precipitation of carbides within the grains [18]. The microstructural analysis of the HAZ in the PWHT low-carbon steel sample quenched in used oil for a few minutes and then slow-cooled in a furnace reveals a complex interplay of bainitic and pearlitic phases. The fine-grained structure with both and more ductile pearlitic regions highlights the effectiveness of the used oil quenching followed by furnace cooling in achieving a balanced microstructure. These findings underscore the importance of controlled cooling rates to optimize the mechanical properties of welded low-carbon steel.

Lastly, as seen in Figure 2c, the WM microstructure of the low-carbon steel, following quenching in unused oil and furnace cooling, shows a predominantly combination of coarse-grained structure and fine grains compared to the base metal and HAZ. This combination of both structures is associated with the solidification zones in the weld pool. During welding, the WMZ solidifies from the outer edges toward the centre of the weld pool. The regions near the fusion line (where the WMZ meets the HAZ) experience slightly lower temperatures than the central area of the weld pool. As a result, these outer regions cool and solidify faster than the centre, leading to finer grains at the edges of the weld bead. The central region of the WMZ, where the temperature is highest, cools more slowly and allows grains to grow larger, resulting in a coarser structure. The micrograph showed that it is characterized by a

predominant Widmanstätten ferrite structure (lighter regions) with some bainitic ferrite (darker regions) and pearlite phase (alternating layers of light + darker regions). The elongated, plate-like grains with a characteristic geometric pattern are indicative of bainitic ferrite. The Widmanstätten ferrite microstructure observed forms during cooling at a relatively slow rate, allowing ferrite to nucleate and grow in a specific crystallographic orientation. Likewise, the WM may have a somewhat higher carbon content due to electrode composition. Increased carbon content can promote the formation of Widmanstätten ferrite, which usually exhibits good strength but can be associated with reduced toughness compared to acicular ferrite. The elongated and feathery regions observed alongside the Widmanstätten ferrite are likely bainitic ferrite. Bainite forms at a faster cooling rate than Widmanstätten ferrite but slower than acicular ferrite. The presence of bainitic ferrite contributes to a balance of strength and ductility in the microstructure. In general, these findings underscore the importance of controlled quenching and cooling processes in optimizing the microstructure and performance of welded low-carbon steel components.

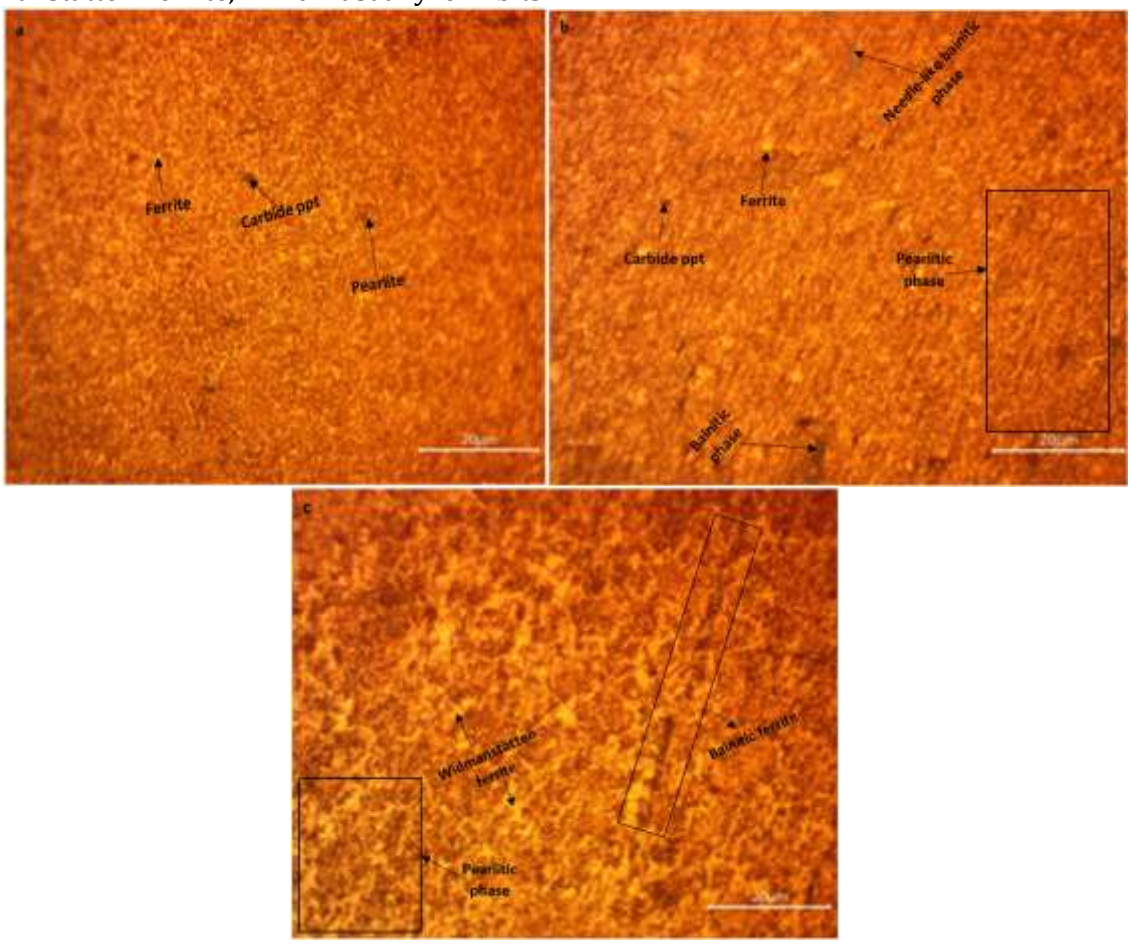

Figure 2: Optical micrograph (a) Base metal of welded low carbon steel. (b) HAZ of welded low carbon steel. (c) WM of welded low carbon steel in un-used oil bath

Figure 3 depicts the microstructure of the base metal, HAZ, and WM, respectively, of samples quenched in a used oil bath for a few minutes and then allowed to cool inside the furnace to room temperature. The base metal (Figure 3a) micrograph comprises predominantly ferrite (light areas) and pearlite (alternating dark and light regions), which were formed during the heat treatment process. Traces of retained austenite (lighter regions) were observed between the pearlite phases. The formation of pearlite and ferrite can both be attributed to

slow cooling in the furnace and the rapid cooling rate during quenching in the used oil. Used oil provides a slower cooling rate than un-used oil due to the potential impurities or breakdown products in the used oil that might introduce minor variations. These variations could manifest as slight changes in grain size or the consistency of the pearlitic transformation. The presence of retained austenite indicates that the cooling rate was not rapid enough to transform all the austenite into either ferrite or pearlite, likely due to the furnace cooling step slowing down the cooling rate after the initial quench and also might be due to contaminants in the used oil bath.

In contrast to the structure observed in Figure 2a, the base metal quenched in used oil in Figure 3a exhibited a predominantly ferritic-pearlitic microstructure. This difference highlights the influence of cooling rate on the resulting microstructure. The slower cooling rate in used oil allowed for the diffusion of carbon atoms and the formation of pearlite, while the faster cooling rate in unused oil led to the formation of both pearlite phases with some traces of carbides. This complex microstructure results from the combined effects of welding, rapid quenching, and slow furnace cooling, influencing the mechanical properties of the base metal, such as hardness and strength. In Figure 3b, the micrograph of the HAZ reveals a coarse microstructure with a predominantly pearlitic structure as compared to Figure 3a, indicated by the dark regions, and lighter regions typically indicate the presence of ferrite as well as retained austenite, a metastable phase that can persist after quenching if the cooling rate is not fast enough or if there are alloying elements that stabilize austenite, as this can be associated with the oil bath that was utilized. The lighter regions are interspersed within the pearlitic matrix, consistent with the typical distribution of ferrite and retained austenite. Traces of carbides were observed within the pearlitic phase, contributing to the overall strength and ductility of the HAZ. This combination of phases results in a balance of hardness, strength, and toughness, crucial for the integrity and performance of the welded joint. Understanding this microstructure helps in optimizing welding parameters and PWHTs to achieve the desired mechanical properties. Furthermore, in Figure 3c, the microstructure of the WM was darker than the previous microstructure and reveals a more predominantly bainitic phase represented by darker regions, a pearlitic phase represented by light and dark regions arranged in alternate layers, and a widmanstätten ferrite structure also seen in Figure 2c, which was represented by much lighter regions with some areas of carbides in the bainitic regions. This is consistent with the expected microstructure of a low-carbon steel weldment quenched in unused oil and cooled in a furnace. Compared to Figure 2c, the microstructure is coarser than that of the WM when quenched in un-used oil. The formation of Widmanstätten ferrite, bainitic and pearlitic phases, and the presence of carbides have been explained in the previous discussion. In general, the WM of the low-carbon steel sample, quenched in an oil bath and cooled in a furnace, displays a complex microstructure consisting of different phases. This combination of phases provides a balance of hardness, strength, and toughness, essential for the integrity and performance of the welded joint. Understanding these microstructural features helps in optimizing welding and PWHT processes to achieve desired mechanical properties.

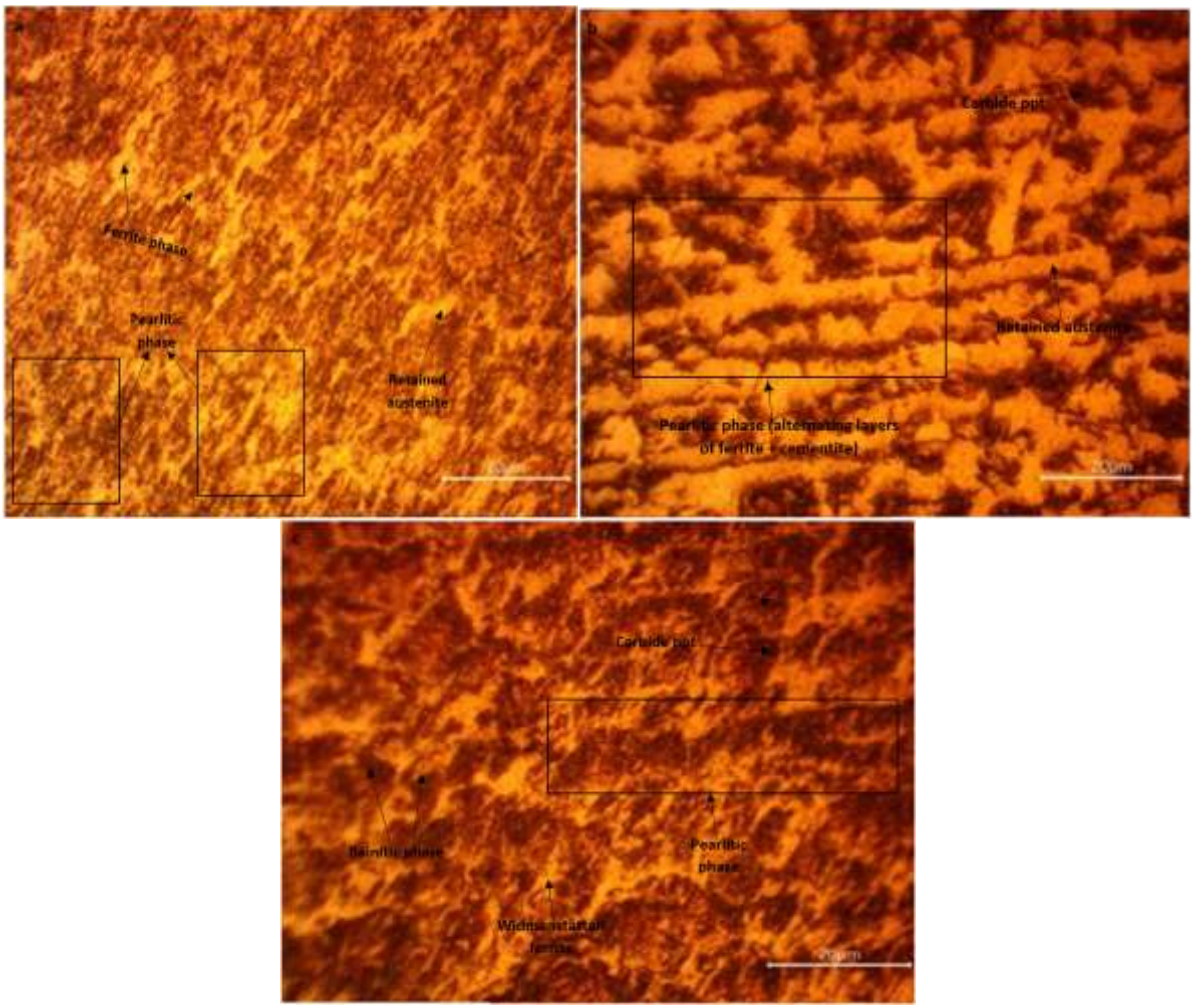

Figure 3: Optical micrograph (a) Base metal of welded low carbon steel. (b) HAZ of welded low carbon steel. (c) WM of welded low carbon steel in used oil bath

In addition, the difference in grain size between samples quenched in used and unused oil is primarily due to the difference in cooling rates. The slower cooling rate in used oil promotes the formation of coarse grains, while the faster cooling rate in unused oil leads to fine grains. This is because used oil typically contains contaminants that reduce its heat transfer efficiency, resulting in a slower cooling rate compared to unused oil. Slower cooling allows for more nucleation sites to form within the material, leading to a smaller number and larger grains, as the slower cooling rate provides more time for atoms to rearrange and form new crystal nuclei.

Tensile properties

The tensile results reveal a nuanced relationship between welded joint design and the resulting mechanical properties (tensile strength and yield strength) of low carbon steel (AISI 1020) welded with E6013 mild steel electrodes using SMAW before PWHT and after PWHT in different media (used and unused oil). The results as seen in Figure 4 reveal distinct trends in the ultimate tensile strength (UTS) of the welded joints based on the type of PWHT and joint design. In terms of joint design effect, the bevel joint consistently exhibited the highest UTS (188.39MPa, 145.49MPa, and 135.91MPa) across all treatment groups which include un-used, used and as-welded, respectively. This is attributed to the bevel joint design, which

maximizes the cross-sectional area of the weld and distributes stress more evenly compared to butt and half-lap joints. The larger weld area reduces stress concentration, resulting in improved tensile strength while the butt joint showed intermediate UTS values. It was noticed that, butt joint offers a larger weld area than half-lap joint but still experiences some stress concentration, particularly, if the weld profile is not reinforced. However, half-lap joint showed the lowest UTS values across all treatment groups. The smaller bonding area and stress concentration at the overlap edge make the half-lap joint more susceptible to failure under tensile loading.

In terms of the post welding heat treatment effect, the unused oil quench produced the highest UTS (188MPa, 164.35MPa, and 158.03MPa) for all joint designs which are bevel, butt and half-lap, respectively. The gradual cooling in unused oil promotes the formation of fine grain martensite, as seen in Figure 6, a hard and brittle microstructure that significantly increases strength. However, this increased strength comes at the cost of reduced ductility and toughness. The used oil quench resulted in intermediate UTS values. The slower cooling rate in used oil leads to the formation of a softer microstructure with some tempered martensite, as presented in Figure 3, offering a balance of strength and ductility, while the as-welded exhibited the lowest UTS values. The as-welded condition typically contains residual stresses and potentially brittle microstructures, which weaken the joint and reduce tensile strength. The results highlight the significant influence of both joint design and PWHT on the tensile strength of welded low-carbon steel. Bevel joints, with their maximized weld area and stress distribution, consistently outperform butt and half-lap joints in terms of UTS. Furthermore, the type of PWHT plays a crucial role in determining the final microstructure and mechanical properties of the weldment. While quenching in unused oil maximizes strength, it also reduces ductility and toughness. In contrast, quenching in used oil offers a compromise between strength and ductility. As-welded joints exhibit the lowest strength due to residual stresses and potentially unfavorable microstructures.

The yield strength results, as depicted in Figure 5, exhibit trends similar to those observed in the tensile strength results shown in Figure 4, with distinct variations based on joint design and PWHT. These findings underscore the critical role of both joint design and PWHT in defining the mechanical behavior of welded low-carbon steel.

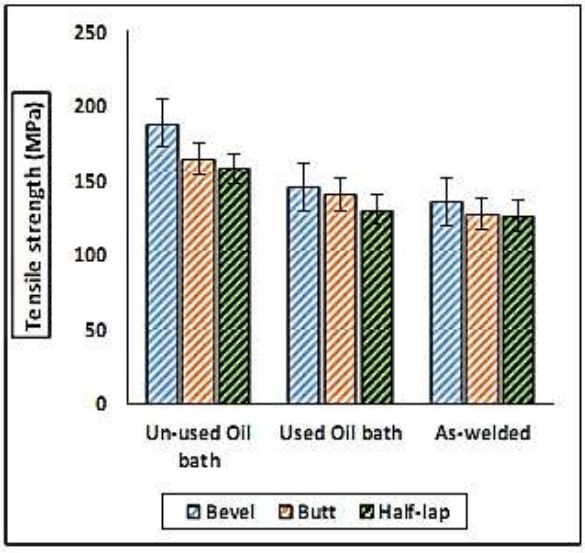

Figure 4: Tensile strength of welded sample before and after PWHT

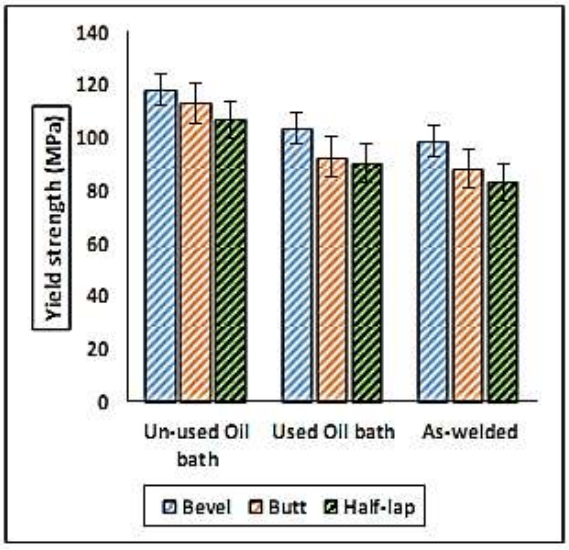

Figure 5: Yield strength of welded sample before and after PWHT

In terms of the joint design influence bevel joints demonstrate superior resistance to yielding due to their optimal stress distribution. Yield strength values for bevel joints are notably higher across each post-weld treatment-unused oil quench (117.98 MPa), used oil quench (103.75 MPa), and as-welded (98.52 MPa). This highlights the bevel joint's capability to manage stress more effectively compared to other joint types. Across the PWHT unused oil quench treatment maximizes yield strength but at the expense of ductility. Yield strengths are highest for unused oil quench across bevel, butt, and half-lap joints (117.98 MPa, 113 MPa, and 107 MPa, respectively). The rapid cooling and subsequent furnace cooling result in a microstructure dominated by hard phases like martensite, enhancing strength but reducing ductility. Used oil quench offers a more balanced approach, the used oil quench achieves moderate yield strengths (103 MPa, 92.74 MPa, and 90.31 MPa for bevel, butt, and half-lap joints, respectively). The presence of contaminants in the used oil results in a more variable cooling rate, producing a mix of hard and tough phases that balance strength and ductility. While as-welded condition exhibit the lowest yield strengths (98.52 MPa for bevel, 88.31 MPa for butt, and 83.31 MPa for half-lap joints). The absence of any heat treatment leaves the microstructure with inherent weaknesses, such as residual stresses and inhomogeneous phase distributions, which adversely affect yield strength. These findings emphasize the importance of careful selection of both joint design and PWHT to tailor the yield strength and overall mechanical performance of welded joints to specific application requirements. Bevel joints are preferable for applications requiring higher yield strength due to their superior stress distribution. For applications necessitating a balance between strength and ductility, the used oil quench treatment is recommended. In contrast, the unused oil quench treatment should be chosen when maximizing yield strength is paramount, albeit with a trade-off in ductility. Finally, as-welded joints, while less optimal in terms of yield strength, might be suitable for applications where post-weld treatments are not feasible or necessary. Overall, the strategic combination of joint design and appropriate PWHT can significantly enhance the mechanical properties of welded low-carbon steel, ensuring optimal performance tailored to the specific demands of the application.

Impact strength

The impact strength results, as seen in Figure 6, highlight the critical role of PWHT in determining the toughness of welded joints, while joint design has a relatively smaller effect. Impact of PWHT showed that in the used oil quench, this method consistently achieved the highest impact strength across all joint designs (65.69 J/mm^2, 57.13 J/mm^2, and 43.83 J/mm^2 for bevel, butt, and half-lap joints, respectively). The slower cooling rate associated with used oil quenching promotes the formation of a tempered microstructure, as illustrated in Figure 3c, which predominantly consists of coarse ferrite and tempered martensite. This microstructure offers a good balance of strength and ductility, enhancing the material's ability to absorb energy upon impact and resist fracture. In the as-welded condition intermediate impact strength was observed across all joints (63.38 J/mm^2, 39.17 J/mm^2, 35.54 J/mm^2 for bevel, butt, and half-lap joints, respectively). As-welded joints typically possess a mixture of microstructures, including some untempered martensite, as shown in Figure 3b, which can be brittle. However, the presence of other ductile phases like pearlite and retained austenite can still contribute to reasonable impact resistance. While unused oil quench treatment showed the lowest impact strength for all joint designs (40.39 J/mm^2, 35.90 J/mm^2, 35.16 J/mm^2 for bevel, butt, and half-lap joints, respectively), rapid quenching in unused oil predominantly results in the formation of martensite, a hard but brittle microstructure. The high hardness of martensite restricts plastic deformation, making the joint susceptible to fracture under impact loading. Furthermore, regarding the impact of joint design, it does not significantly influence the ranking of impact strength within each PWHT group, some minor differences can be observed. Bevel joints generally show slightly higher impact strength compared to butt and half-lap joints within each PWHT group. This is likely due to the larger weld area and better

stress distribution in bevel joints, which can delay the initiation and propagation of cracks under impact loading. Butt joint exhibits intermediate impact strength, generally falling between bevel and half-lap joints while half-lap joints consistently show the lowest impact strength within each PWHT group. The smaller bonding area and stress concentration at the overlap make it the weakest point, prone to fracture under impact. The impact strength results emphasize the importance of PWHT in optimizing the toughness of welded low-carbon steel joints. Quenching in used oil, with its associated slower cooling rate and tempered microstructure, consistently produces the highest impact strength. As-welded joints offer intermediate impact resistance while quenching in unused oil led to a predominantly martensitic microstructure that significantly reduces impact toughness. While joint design plays a less dominant role in determining impact strength compared to PWHT, it still influences the overall performance of the welded joint. Bevel joints generally exhibit slightly better impact resistance than butt and half-lap joints due to their superior stress distribution. These findings highlight the necessity of carefully selecting both PWHT and joint design to achieve the desired combination of strength and toughness for specific applications.

Hardness

The hardness, which is the resistance to indentation, is presented in Figure 7 for different zones of each welded joint across each heat-treatment. The hardness values ranged between 63.5 HV and 76.5 HV across the zones of the welded samples. The base metal hardness for as-welded state exhibited a hardness of 63.5 HV. While for the PWHT in both oil baths, the hardness increased to 65.1 HV for the used oil quench and 65.3 HV for the unused oil quench.

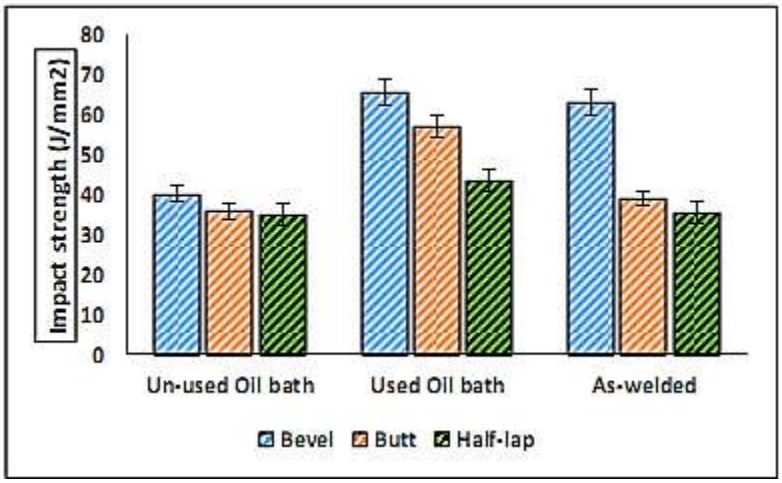

Figure 6: Impact strength of welded sample before and after PWHT

The highest hardness in the unused oil quenched sample, indicating a 3% increment, is attributed to the presence of martensite in the microstructure, as seen in Figures 2a and 3a. In the HAZ it consistently showed higher hardness compared to the WM and base metal across all joints and post-weld treatments. This increase in hardness is due to the rapid heating and cooling cycles during welding, which lead to the formation of martensite, a very hard and brittle phase of steel. The rapid cooling rate in the HAZ, especially near the fusion line, does not allow enough time for the softer ferrite and pearlite phases to form, resulting in a higher concentration of martensite. In addition, the HAZ experiences grain refinement due to the rapid thermal cycles. While smaller grains can improve strength and toughness to some extent, they also contribute to increased hardness, especially when combined with martensite formation. In terms of joint design and hardness, the butt joint had the highest hardness which was found in the HAZ of the oil-quenched butt joint (76.5 HV). This is because the butt joint

configuration leads to more concentrated heat input and faster cooling rates compared to bevel and half-lap joints. The rapid cooling in the butt joint HAZ promotes a greater degree of martensite formation, resulting in higher hardness. In the bevel joint the HAZ of the bevel joint quenched in an unused oil bath showed slightly lower hardness (75.4 HV) due to more gradual heat dissipation and slower cooling rates. While in the half-lap joint quenched in an unused oil bath, with its wider HAZ and even slower cooling, had the lowest hardness (74.6 HV) among the three joint types quenched in un-used oil. The same trend was observed for joints quenched in used oil bath, with the butt joint having the highest hardness (75.8 HV), followed by the bevel joint (74.7 HV), and the half-lap joint (73.8 HV). In as-welded state when comparing each joint in the as-welded state, the same trend was observed: the butt joint exhibited the highest hardness (75.7 HV), followed by the bevel joint (74.5 HV), and the half-lap joint (73.5 HV). Also, the in the WM hardness zone the butt joint had the highest hardness among other joints both before (74 HV) and after PWHT (74.6 HV), the bevel joint showed an increase in hardness from 73.8 HV before PWHT to 74.5 HV after PWHT and half-lap joint had the lowest hardness, with 72.1 HV before PWHT and 73.2 HV after PWHT.

In general, across all weld regions (base metal, HAZ, and WM) and PWHT conditions, the hardness decreases from the butt joint to the bevel joint to the half-lap joint. This trend suggests that for applications requiring high hardness, butt joints are the most suitable, while bevel joints can be applied in applications needing moderate hardness. Half-lap joints, having the lowest hardness, might be selected for applications where lower hardness is acceptable or advantageous.

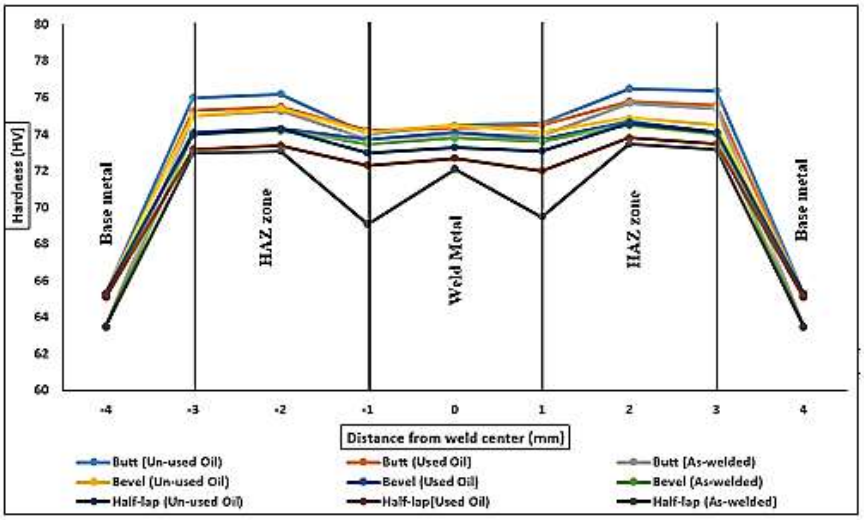

Figure 7: Hardness welded sample before and after PWHT

These findings emphasize the importance of selecting the appropriate joint design and PWHT to achieve the desired hardness and mechanical properties for specific applications.

Cooling rate influence and oil properties

The quenching media used (unused and used oil) played a significant role in determining the mechanical properties of the low-carbon steel samples after PWHT due to the chemical composition of the media as stated by Almostaneer *et al.* [36] as well as changed in the viscosity and lubricity [37] and thermal conductivity. The unused oil bath, being fresh, had lower viscosity and higher thermal conductivity compared to the used oil bath, leading to faster cooling rates. This rapid cooling induced the formation of finer martensitic structures, resulting in the higher tensile strength and yield strength observed in the

bevel joint quenched in unused oil as explained above. Conversely, the used oil, having been exposed to previous quenching cycles as well as usage, exhibited higher viscosity, reduced thermal conductivity and lower lubricity [37] due to the accumulation of contaminants and degradation products, which can lead to increased friction and heat during welding, potentially resulting in lower mechanical performance compared to that of the unused oil bath. This slowed the cooling process, promoting the formation of a coarser, tempered martensite or bainite structure. This explains the lower tensile and yield strengths but higher impact strength as observed in the samples quenched in used oil above. The slower cooling allowed for greater ductility, improving the toughness and ability of the material to absorb energy during impact. The observed differences in mechanical behavior between the two oil baths underscore the importance of quenching medium properties on the microstructure and mechanical properties of the steel. Faster cooling generally favors strength, while slower cooling enhances toughness and ductility.

Conclusion

The investigation into the effect of weld joints and PWHT on the mechanical properties of low-carbon steel (AISI 1020) using SMAW with E6013 electrodes successfully achieved its objectives. The study established a clear correlation between joint design, PWHT, resulting microstructure, and mechanical performance. Notably, the samples quenched in the unused oil bath consistently exhibited higher mechanical properties, including UTS and yield strength, compared to those quenched in the used oil bath. The bevel joint quenched in unused oil demonstrated the highest UTS (188.39 MPa) and yield strength (117.98 MPa), highlighting that the faster cooling rate in the unused oil bath promoted a finer microstructure, which contributed to enhanced strength. In contrast, the samples quenched in used oil, which cooled more slowly, exhibited lower tensile and yield strengths due to coarser microstructures, typically associated with reduced strength. Among the joints, the bevel joint also emerged as a prime candidate for applications prioritizing high tensile and yield strengths, while the butt joint quenched in used oil demonstrated superior impact strength (65.69 J/mm^2). This increased impact strength is attributed to the tempered microstructure formed during the slower cooling process, resulting in a better balance of strength and ductility. Additionally, the butt joint quenched in unused oil exhibited the highest hardness (76.5 HV) in the HAZ, illustrating the potential for localized hardening through specific PWHT conditions. These findings underscore the critical role of both joint design and cooling rate (determined by oil bath conditions) in influencing the mechanical properties of low-carbon steel welds. Tailoring both welding and heat treatment procedures is essential to achieving desired mechanical properties for specific applications. Future research could further investigate the effects of varying bevel angles, other joint designs, and alternative PWHT methods to optimize mechanical properties for a broader range of materials and applications.

Acknowledgements

The authors would like to thank the Department of Metallurgical and Materials Engineering at the Federal University of Technology Akure for providing access to their laboratories, which facilitated the execution of several methodologies in this study.

Funding

This study did not receive any specific grant from funding agencies in the public, commercial, or not-for-profit sectors.

Conflict of Interest

No conflicts of interest declare that there is no conflict of interest in this study.

ORCID

Isiaka Oluwole Oladele
https://orcid.org/0000-0001-7168-1518
Samuel Olumide Falana
https://orcid.org/0000-0002-2938-0305
Collins Chidiebere Okoye

https://orcid.org/0009-0002-2963-3867
Peace Pamilerin Adara
https://orcid.org/0000-0001-7029-6220
Adesuyi Kole Aladenika
https://orcid.org/0009-0007-3765-7400
Sunday Gbenga Borisade
https://orcid.org/0000-0002-7218-8773

Reference

[1]. S.I. Talabi, O.B. Owolabi, J.A. Adebisi, T. Yahaya, Effect of welding variables on mechanical properties of low carbon steel welded joint, *Advances in Production Engineering & Management*, **2014**, *9*, 181-186. [Crossref], [Google Scholar], [Publisher]
[2]. D. Sumardiyanto, E. Susilowati, Effect of welding parameters on mechanical properties of low carbon steel API 5L shielded metal arc welds, *American Journal of Materials Science*, **2019**, *9*, 15–21. [Google Scholar]
[3]. I.O. Oladele, D.B. Alonge, T.O. Betiku, A.A. Barnabas, S. Shittu, Distinctiveness of welding joints design based on mechanical and corrosion environmental influence on low carbon steel, *Advanced Technologies and Materials*, **2019**, *44*, 13-19. [Crossref], [Google Scholar], [Publisher]
[4]. B.K. Singh, A.K. Jha, P.K. Singh, Effects of joint geometries on welding of mild steel by shielded metal arc welding (SMAW). *International Research Journal of Engineering and Technology*, **2015**, *2*, 1-7. [Google Scholar], [Publisher]
[5]. J. da Cruz Payão Filho, E. Kimus Dias Passos, R. Stohler Gonzaga, D. Drumond Santos, V. Pereira Maia, D. Russo Juliano, The influence of the welding process on the ultrasonic inspection of 9% Ni steel pipe circumferential welded joints, *Materials*, **2020**, *13*, 961. [Crossref], [Google Scholar], [Publisher]
[6] F. Ata, A. Calık, N. Ucar, Investigation on the microstructure and mechanical properties of ASTM A131 steel manufactured by different welding methods, *Advances in Materials Science*, **2022**, *22*, 32-40. [Crossref], [Google Scholar], [Publisher]
[7]. C. González-González, J. Los Santos-Ortega, E. Fraile-García, J. Ferreiro-Cabello, Environmental and economic analyses of tig, mig, mag and smaw welding processes, *Metals*, **2023**, *13*, 1094. [Crossref], [Google Scholar], [Publisher]
[8]. Z. Zhang, Y. Ma, S. Liu, L. Su, L. Fletcher, H. Li, B. Wang, H. Zhu, inhomogeneous strain behaviors of the high strength pipeline girth weld under longitudinal loading, *Materials*, **2024**, *17*, 2855. [Crossref], [Google Scholar], [Publisher]
[9]. H. Alipooramirabad, N. Cornish, R. Kurji, A. Roccisano, R. Ghomashchi, Quenched and tempered steels welded structures: Modified gas metal arc welding-pulse vs. shielded metal arc welding, *Metals*, **2023**, *13*, 887. [Crossref], [Google Scholar], [Publisher]
[10]. P. Purtscher, S. Sheng, T. Dickson, Analysis of circumferential welds in bwrs for life beyond 60, pressure vessels and piping conference, *American Society of Mechanical Engineers*, **2015**, V007T007A023. [Crossref], [Google Scholar], [Publisher]
[11]. A. Singh, N.K. Grover, Weld properties of low carbon steel using shielded metal arc welding, *Applied Mechanics and Materials*, **2015**, *813*, 486-490. [Crossref], [Google Scholar], [Publisher]
[12]. P.K. Baghel, Effect of SMAW process parameters on similar and dissimilar metal welds: An overview, *Heliyon*, **2022**, *8*. [Google Scholar], [Publisher]
[13]. P. Senthilkumar, Exploration of tensile properties of low carbon steel welded joint, *International Journal of Scientific Research in Science, Engineering and Technology (IJSRSET)*, **2021**, *8*, 49–55. [Crossref], [Google Scholar], [Publisher]
[14] J.C. Jorge, O. Meira, F. Madalena, L. de Souza, L. Araujo, M. Mendes, Evaluation of the AISI 904L alloy weld overlays obtained by GMAW and electro-slag welding processes, *Journal of Materials Engineering and Performance*, **2017**, *26*, 2204-2212. [Crossref], [Google Scholar], [Publisher]
[15]. M. Fitri, P. Hidayatullah, K.M. Wibowo, A.S. Darmawan, The effect of smaw welding currents on mechanical properties and micro structures of low carbon steels, materials science forum, *Trans Tech Publ*, **2021**, 15-23. [Crossref], [Google Scholar], [Publisher]
[16]. Q.H. Ismael, Investigation of mechanical properties of low carbon steel weldments for different welding processes, *SVU-International Journal of Engineering Sciences and Applications*,

2022, *3*, 116-122. [Crossref], [Google Scholar], [Publisher]
[17]. R. Jha, A. Jha, Influence of welding current and joint design on the tensile properties of SMAW welded mild steel joints, *International Journal of Engineering Research and Applications*, **2014**, *4*, 106-111. [Google Scholar], [Publisher]
[18]. I.O. Oladele, D.B. Alonge, T.O. Betiku, E.O. Igbafen, B.O. Adewuyi, Performance evaluation of the effects of post weld heat treatment on the microstructure, mechanical and corrosion potentials of low carbon steel, *Advanced Technologies and Materials*, **2019**, *44*, 41-46. [Crossref], [Google Scholar], [Publisher]
[19]. Y. Shuaib-Babata, R. Adewuyi, J. Aweda, Effects of thermal treatment processes (TTP) on some of the mechanical properties of welded 0.165% carbon steel, *Journal of Production Engineering,(JPE)*, **2017**, *20*. [Crossref], [Google Scholar], [Publisher]
[20]. O. Ajide, O. Anifalaje, I. Akande, F. Musa, O. Fayomi, O. Oluwole, K. Oluwasegun, O. Ajao, Effect of post-weld heat-treatment on corrosion and microstructure properties of electric arc weldedmild steels, *Portugaliae Electrochimica Acta*, **2023**, *56*, 9-29. [Crossref], [Google Scholar], [Publisher]
[21]. M.Y. Samir, Investigation on effect of welding current and post weld heat treatment on mechanical properties of weldment of low carbon steel. *International Journal of Research in Engineering and Technology*, **2015**, *4*, 54–58. [Publisher]
[22] R.P. Adebare, P.K. Edward, Impact of Post-Weld Heat Treatment (PWHT) on the Hardness and Microstructure of Low Carbon Steel, International J. Innov. Sci. Eng. Technol., **2016**, 3, 16–26. [Google Scholar]
[23]. E. Harati, E. Harati, U. Onochie, Effect of post-weld heat treatment on mechanical and microstructural properties of high strength steel weld metal, *Welding International*, **2024**, *38*, 422-429. [Crossref], [Google Scholar], [Publisher]
[24]. H.W. Lee, K.J. Yoo, M.T. Tran, I.Y. Moon, Y.-S. Oh, S.-H. Kang, D.-K. Kim, Effect of quenching tempering-post weld heat treatment on the microstructure and mechanical properties of laser-arc hybrid-welded boron steel, *Materials*, **2019**, *12*, 2862. [Crossref], [Google Scholar], [Publisher]
[25]. R.K. Aninda, S.M. Karobi, R. Shariar, M.M. Rahman, M.I.I. Rabby, Effect of post-weld heat treatment on mechanical properties and microstructure in electric arc welded mild steel joints, *Journal of Engineering Research*, **2024**, *12*, 210-215. [Crossref], [Google Scholar], [Publisher]
[26] A. Reyes, E. Bedolla, R. Perez, A. Contreras, Effect of heat treatment on the mechanical and microstructural characterization of Mg-AZ91E/TiC composites, *Composite Interfaces*, **2018**, *24*, 346–354. [Crossref], [Google Scholar], [Publisher]
[27]. M.M. Gad, A. Rahoma, A.M. Al-Thobity, A.S. ArRejaie, Influence of incorporation of ZrO_2 nanoparticles on the repair strength of polymethyl methacrylate denture bases, *International Journal of Nanomedicine*, **2016**, 5633-5643. [Crossref], [Google Scholar], [Publisher]
[28]. M.M.A. Gad, R. Abualsaud, A.M. Al-Thobity, D.F. Almaskin, Z.A. AlZaher, T.H. Abushowmi, M.S. Qaw, S. Akhtar, F.A. Al-Harbi, Effect of SiO_2 nanoparticles addition on the flexural strength of repaired acrylic denture base, *European Journal of Dentistry*, **2020**, *14*, 019-023. [Crossref], [Google Scholar], [Publisher]
[29]. M. Momeni, M. Guillot, Post-weld heat treatment effects on mechanical properties and microstructure of AA6061-T6 butt joints made by friction stir welding at right angle (RAFSW), *Journal of Manufacturing and Materials Processing*, **2019**, *3*, 42. [Crossref], [Google Scholar], [Publisher]
[30]. M. Kim, H. Kim, J. Han, J. Lee, Y. Kim, N. Kang, M. Kang, C. Kim, Influence of backing materials towards the fatigue strength of butt-welded joints, *Proceedings of the Institution of Mechanical Engineers, Part C: Journal of Mechanical Engineering Science*, **2011**, *225*, 1798-1807. [Crossref], [Google Scholar], [Publisher]
[31]. Z. Zhu, Y. Li, M. Zhang, C. Hui, Effects of stress concentration on the fatigue strength of 7003-T5 aluminum alloy butt joints with weld reinforcement, *International Journal of Modern Physics B*, **2015**, *29*, 1540023. [Crossref], [Google Scholar], [Publisher]

[32]. N. Mamatha, P.K. Madineni, R. Sisir, S. Sravani, S. Nallamilli, J.R. Jyothy, Evaluation of transverse strength of heat cure denture bases repaired with different joint surface contours: an in vitro study, The *Journal of Contemporary Dental Practice*, **2020**, *21*, 166-170. [Google Scholar], [Publisher]
[33]. S.A. Antonson, A.R. Yazici, Z. Okte, P. Villalta, D.E. Antonson, P.C. Hardigan, Effect of resealing on microleakage of resin composite restorations in relationship to margin design and composite type, *European Journal of Dentistry*, **2012**, *6*, 389-395. [Google Scholar], [Publisher]
[34]. C. Song, B. Xing, X. He, S. Wang, Self-piercing riveting for single-strap butt joints in similar aluminium alloys, *Science and Technology of Welding and Joining*, **2021**, *26*, 301-308. [Google Scholar], [Publisher]
[35]. M. Dodo, T. Ause, M. Adamu, Y. Ibrahim, Effect of post-weld heat treatment on the microstructure and mechanical properties of arc welded medium carbon steel, *Nigerian Journal of Technology*, **2016**, *35*, 337-343. [Crossref], [Google Scholar], [Publisher]
[36]. H. Almostaneer, C. Cadigan, S. Liu, D.L. Olson, R. Richards, H.J. Liang, Hydrocarbon–metal reactions during metal arc welding under oil (MAW-UO), *Science and Technology of Welding and Joining,* **2011**, *16*, 619-629. [Crossref], [Google Scholar], [Publisher]
[37]. M. Sejkorová, P. Hurtová I, Jilek, M. Novák, O. Voltr, Study of the Effect of Physicochemical Degradation and Contamination of Motor Oils on Their Lubricity, *Coatings*, **2021**, *11*, 60. [Crossref], [Google Scholar], [Publisher]